Front. Earth Sci. 2024, 18(3): 598–610
https://doi.org/10.1007/s11707-022-0978-1

RESEARCH ARTICLE

Storage, pattern and driving factors of soil organic carbon in the desert rangelands of northern Xinjiang, north-west China

Huixia LIU[1], Zongjiu SUN (✉)[1,2,3], Yuxuan CUI[1], Yiqiang DONG[1,2,3], Panxing HE[1], Shazhou AN[1,2,3], Xianhua ZHANG[1,2,3]

1 College of Grassland Sciences, Xinjiang Agricultural University, Urumqi 830052, China
2 Ministry of Education Key Laboratory for Western Arid Region Grassland Resources and Ecology, Urumqi 830052, China
3 Xinjiang Key Laboratory of Grassland Resources and Ecology, Urumqi 830052, China

Abstract Soil organic carbon (SOC) is a critical variable used to determine the carbon balance. However, large uncertainties arise when predicting the SOC stock in soil profiles in Chinese grasslands, especially on desert rangelands. Recent studies have shown that desert ecosystems may be potential carbon sinks under global climate change. Because of the high spatial heterogeneity, time-consuming sampling methods, and difficult acquisition process, the relationships the SOC storage and distribution have with driving factors in desert rangelands remain poorly understood. Here, we investigated and developed an SOC database from 3162 soil samples (collected at depths of 0–10 cm and 10–20 cm) across 527 sites, as well as the climate conditions, vegetation types, and edaphic factors associated with the sampling sites in the desert rangelands of northern Xinjiang, north-west China. This study aims to determine the SOC magnitude and drivers in desert rangelands. Our findings demonstrate that the SOC and SOC density (SOCD) were 0.05–37.13 $g \cdot kg^{-1}$ and 19.23–9740.62 $g \cdot m^{-2}$, respectively, with average values of 6.81 ± 5.31 $g \cdot kg^{-1}$ and 1670.38 ± 1202.52 $g \cdot m^{-2}$, respectively. The spatial distributions of SOC and SOCD all showed gradually decreasing trends from south-west to north-east. High-SOC areas were mainly distributed in the piedmont lowlands of the Ili valley, while low-SOC regions were mainly concentrated in the north-west area of Altay. The redundancy analysis results revealed that all environmental factors accounted for approximately 37.6% of the spatial variability in SOC; climate factors, vegetation factors, and soil properties explained 15.0%, 1.7%, and 12.3%, respectively. The structural equation model (SEM) further indicated that evapotranspiration, average annual precipitation, and the SWC were the dominant factors affecting SOC accumulation, mainly through direct effects, although indirect effects were also delivered by the vegetation factors. Taken together, the results obtained herein updated the SOC data pool available for desert rangelands and clarified the main driving factors of SOC variations. This study provided supporting data for the sustainable use and management of desert rangelands and the global ecosystem carbon budget.

Keywords soil organic carbon, desert rangeland, SEM analysis, driving factors, Xinjiang Uygur Autonomous Region of China

1 Introduction

Soil represents the largest carbon pool in Earth's terrestrial ecosystem and contributes considerably to the global carbon (C) balance (Lal, 2004). Compared to the vegetation and atmospheric carbon pools, the soil organic carbon (SOC) storage is 2–3 times higher in terrestrial ecosystems (Scharlemann et al., 2014). Thus, a small proportion of soil C loss may increase the atmospheric carbon dioxide (CO_2) concentration (Bradford et al., 2016), leading to global climate anomalies (Chen et al., 2016; Lal, 2019). To date, many studies have reported that SOC storage is mainly concentrated in steppes (Li et al., 2018a), meadows (Ma et al., 2020), alpine meadows (Guan et al., 2018), farmlands (Ghimire et al., 2019), and wetlands (Wang et al., 2020). However, there is a lack of knowledge regarding the carbon status in desert rangelands, where harsh ecological-environmental conditions, sparse vegetation, poor soil, relatively low

Received August 3, 2021; accepted February 21, 2022

E-mail: nmszj@21cn.com

SOC contents, and relatively low productivity occur (Su et al., 2015). As a result, the carbon storage function of desert rangelands has been ignored and underestimated for a long time, and existing research on this topic has been relatively weak (Wang et al., 2010; Germano et al., 2011). Simultaneously, published research has emphasized that SOC sequestration is determined by different climatic conditions (Chen et al., 2020; Lei et al., 2020), land use patterns (Illiger et al., 2019), topographic factors (Zhu et al., 2017), and soil types (Bruun et al., 2015). However, little work has focused on changes in the SOC among different soil matrix subclasses of the same grassland, especially desert rangelands. At the same time, the expansion of drylands caused by climate change and human activities leads to decreased carbon stocks, regional warming, and land desertification and increases the uncertainty of grassland carbon dynamics (Huang et al., 2015). Therefore, it is necessary to accurately estimate SOC stocks and their changes to support improved carbon management and climate change mitigation measures (Scharlemann et al., 2014).

Desert ecosystems are an important part of terrestrial ecosystems and occupy more than 30% of the land surface; the carbon storage of desert ecosystems is near 8% of the global carbon storage (Li et al., 2015). Deserts are typical ecologically fragile areas that are extremely sensitive to global climate change. The complex environment in desert areas leads to obvious productivity, species composition, and soil matrix variations (Xu, 1993), which in turn result in the high spatial heterogeneity of SOC. Some researchers have pointed out that the contribution of desert ecosystems to the terrestrial carbon cycle is almost negligible (Li et al., 2003). Others have claimed that although the coverage of desert vegetation communities is low, desert regions are widely distributed, and applicability of their carbon storage for decelerating global climate change cannot be ignored (Wang et al., 2014). Moreover, the majority of previous results have indicated that desert areas absorb large amounts of CO_2 in the air at a slow rate (Huo et al., 2018), and many researchers believe that desert ecosystems may be able to serve as long-sought "carbon sinks" for the global carbon cycle (Stone, 2008; Evans et al., 2014). As an important area for CO_2 fixation in the future, desert rangelands have attracted increasing attention from scholars, but strong evidence is still lacking. Some researchers have pointed out that the SOC content in the north-west desert steppe (at soil depths of 0−10 cm) was between 4.03 and 4.67 $g \cdot kg^{-1}$ (Yang and Liu, 2019), while the SOC content in the northern semiarid sandy rangelands was higher than 2.31 $g \cdot kg^{-1}$ (Liu et al., 2013). Yang et al. (2019) indicated that the average SOC density (SOCD) of the desert steppe ecosystems in northern China was 2.51 $kg \cdot C \cdot m^{-2}$ (2000−2017), with an average annual increase of 27.58 $g \cdot m^{-2}$, indicating that the studied desert ecosystem has always been a net carbon sink (Li et al., 2015). Although various lines of evidence support the existence of substantial carbon sinks in desert ecosystems, data confirming these carbon sinks are still limited at present (Petrie et al., 2015).

Most researchers have considered rangelands as a whole when studying SOC and its relationship with environmental factors (Ghimire et al., 2019), but the differences in SOC that exist among different rangeland types and their environmental implications have rarely been examined. At the same time, during the soil evolution process, the main factors controlling the desert rangeland SOC vary depending on the complexity of the environment (Chen et al., 2016; Alidoust et al., 2018; Li et al., 2018b), even in the same area. Thus, the differences in these factors (soil textures, vegetation types, climatic conditions, and human disturbances) lead to a great deal of uncertainty in overall assessments of China's carbon stocks (Delgado-Baquerizo et al., 2017; Alidoust et al., 2018; Wang et al., 2019) and show that no environmental factor can affect SOC as an independent parameter (Hu et al., 2018). In analyses combining these factors, few researchers have quantified the explanation of environmental factors for SOC variation (Zhao et al., 2017). It is of great significance for sustainable land management and accurately predicting SOC stocks to quantify the effects of environmental factors (Lal, 2004). Moreover, the soil carbon storage of desert ecosystems has not yet been comprehensively evaluated, and the SOC driving factors are still unclear. Globally, SOC storage has been linked to climate conditions, vegetation factors, soil properties, and physicochemical factors (such as the soil texture and soil type) (Su et al., 2015). Many studies have reported that climate factors appear to be strongly associated with SOC storage at the national and global scales; specifically, the mean annual precipitation (MAP) has a more notable impact than the mean annual temperature (MAT) (Tang et al., 2018). Therefore, we hypothesized that climate factors (especially MAP) are the main driving factors affecting SOC in desert ecosystems. To test this hypothesis and improve our understanding of SOC accumulation in desert regions, we collected 3162 soil samples (at depths of 0−10 cm and 10−20 cm) from 527 sites in the desert rangelands of northern Xinjiang, northwest China, in 2017−2019. The SOC, pH, electrical conductivity (EC), and bulk density (BD) were analyzed, and climate data (including the MAT, MAP, and $\geqslant$ 10°C annual accumulated temperature) were collected. We revealed and quantified the relationships between environmental factors (climate, vegetation, and soil physical and chemical properties) and SOC through structural equation modeling. Specifically, the objectives of this study were (i) to evaluate the status and spatial distribution of SOC and SOCD in desert rangelands; (ii) to explore the effect of climate, vegetation, and soil properties on SOC storage; and (iii) to reveal the key driving factors affecting the spatial variations in SOC.

The results of this study can help us obtain better quantitative predictions of SOC storage in the future and provide a scientific basis for evaluating ecological restoration practices and soil carbon management to promote sustainable development.

2 Materials and methods

2.1 Overview of the study area

The study area was located in the northern part of the Xinjiang Uygur Autonomous Region of China (latitude 42.14°–48.05° N, longitude 80.61°–95.92° E, elevation range −100 to 2000 m; Fig. 1), the center of Eurasia. The climate characteristics belong to the temperate continental arid and semiarid climate types. The annual precipitation is below 200 mm, and the ⩾ 10°C annual accumulated temperature is 3000°C–3500°C. According to the taxonomy established by the Food and Agriculture Organization/United Nations Educational, Scientific and Cultural Organization (FAO/UNESCO), the soil types in the study area include aridisols and entisols and can be divided into gray desert soils and gray–brown desert soils (from the China soil classification system). The rangeland is dominated by small arbors and shrubs, such as *Haloxylon ammodendron*, *Haloxylon persicum*, *Calligonum leucocladum*, *Tamarix ramosissima*, *Ephedra przewalskii*, and *Sarcozygium xanthoxylum,* and by semishrubs, such as *Ceratoides latens*, *Nanophyton erinaceus*, *Sympegma regelii*, *Reaumuria soongarica*, *Anabasis brevifolia*, *Anabasis salsa*, *Salsola orientalis*, *Salsola arbuscula*, *Seriphidium borotalense*, *Seriphidium terraealbae*, *Seriphidium gracilescens*, *Seriphidium transiliense*, and *Kalidium foliatum*; additionally, there are a few forbs, such as *Petrosimonia sibirica*, *Ceratocarpus arenarius*, and *Halogeton glomeratus*. Therefore, according to the soil matrix and vegetation type information, the analyzed desert rangelands can be divided into sandy desert, gravelly sandy desert, gravelly desert, soil desert, and saline desert types (Xu, 1993).

2.2 Plot selection and field sampling

Based on the distributions delineated in China's Vegetation Atlas at the 1:1000000 scale (Zhang et al., 2007) and the 1:1000000 rangeland type map of Xinjiang published in the 1980s (Xu, 1993), we selected desert rangeland sampling sites across northern Xinjiang according to the representativeness of the vegetation types. Overall, 527 sampling sites were established (Fig. 1), including 87 sandy desert sites, 58 gravelly sandy desert sites, 168 gravelly desert sites, 202 soil desert sites, and 12 saline desert sites. All of the field measurements were conducted at the aboveground biomass peak from July to September between 2017 and 2019.

At each site, we first conducted a detailed investigation of the longitude, latitude, elevation, soil matrix, community name, utilization mode, and intensity information of the desert rangelands. Then, one typical 100 m × 100 m plot was established, and 9 herb subplots (1 m × 1 m) were measured within each plot while another 5 subplots (10 m × 10 m) were measured if the plot contained small arbors or shrubs.

The species composition, height, coverage, plant density, and aboveground biomass were investigated at each site (Fig. 1). The height and plant density were determined by the direct measurement method (Fang et al., 2007). The aboveground biomass was determined by the weighing method (Fang et al., 2007). The vegetation coverage was measured by the visual evaluation

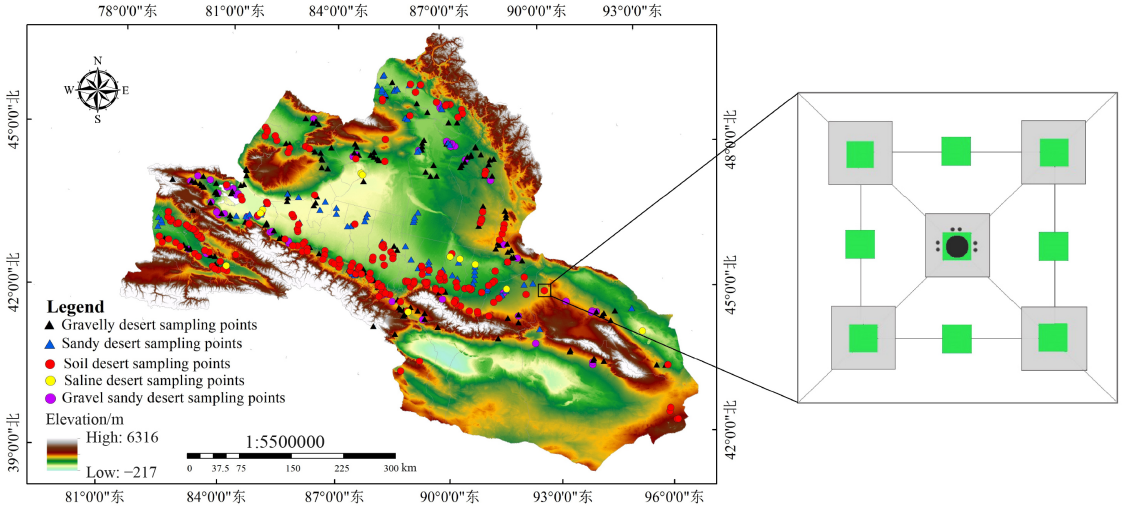

Fig. 1 Geographical location, sample point distribution, and sample layout in northern Xinjiang (n = 527). ■ 10 m × 10 m shrub plot; 1 m × 1 m herb plot; ● 1 m × 1 m soil profile; ⁘ soil nutrient samples and bulk density collection points.

method (Yang et al., 2021). After measuring the aboveground biomass of herbaceous and shrub plots, a soil profile (1 m × 1 m × 1 m) was excavated in the center of each plot (Fig. 1). Soil samples were obtained from three vertical sections (at depths of 0−10 cm and 10−20 cm) by cutting soil blocks (Bao, 2000). At the same time, we used a cutting ring (a stainless-steel cylinder with a volume of 100 cm^3) to collect the soil bulk densities at the corresponding soil layers. We then carried the soil samples back to the laboratory. In total, we collected 3162 soil nutrient samples and 3162 soil bulk density samples (527 sites × 3 soil profiles × 2 soil layers).

2.3 Laboratory analyses

In the laboratory, the soil samples were air-dried after visible plant roots, gravel, and other debris were removed. Each dried soil sample was passed through a 0.25-mm mesh sieve before determining the SOC concentration. The SOC content was measured using the Walkley-Black dichromate oxidation method (Bao, 2000). The soil samples were passed through a 1-mm mesh sieve to measure the soil pH and electrical conductivity using the potentiometer and conductivity methods, respectively (Bao, 2000). The soil bulk density samples were determined using the drying method (105°C, 24 h) (Bao, 2000); then, a 2-mm mesh sieve was used to screen out the gravel, and the samples were washed, dried, and weighed. Then, we used the ratio of the gravel mass to the dry bulk density to calculate the soil-rock ratio.

2.4 Calculation formula

We calculated the SOC density (*SOCD*, in g C·m^{-2}) of each soil sample using the following equation:

$$SOCD = \sum_{i=1}^{n} (1-\theta_i) \times BD_i \times SOC_i \times T_i \times 10, \quad (1)$$

where *SOCD* represents the soil organic carbon density (g·m^{-2}); *SOCi*, BD_i, T_i, θ_i are the organic carbon content (g·kg^{-1}), soil bulk density (g·cm^{-3}), thickness (cm), and mass proportion of the fraction (> 2 mm) in soil layer *I*, respectively; and 10 is the unit conversion factor:

$$CV = \frac{SD}{\text{Mean}} \times 100\%, \quad (2)$$

in the above formula, *CV* represents the coefficient of variation; *SD* represents the standard deviation of the SOC content (g·kg^{-1}) or density data (g·m^{-2}); and Mean represents the average value of the SOC content (g·kg^{-1}) or density (g·m^{-2}).

2.5 Environmental data

To analyze the key driving factors of SOC, some climatic and environmental parameters were obtained at the 527 sampling sites. Climatic variables can exert a lagged accumulative effect on soil C storage (Delgado-Baquerizo et al., 2017), so multiple-year averages were used to explore the effects of these factors on the soil carbon storage. The average values (derived over 1 km × 1 km spatial grid data) of the long-term observed meteorological data were gathered from the National Meteorological Observatory (1957−2018) (Xu et al., 2019). Then, the meteorological data representing each sampling point were acquired by interpolation to indicate the climatic conditions at the actual sampling points (such as annual accumulated temperature ⩾ 10°C, MAT, and MAP).

A land evaporation data set (2000−2018 GLEAM V3) of satellite observations was obtained from the organization website, a vector data image of the study area was clipped, a raster fishing net was created, and evapotranspiration data of the sampling points were acquired (Brecht et al., 2016). Based on sun chlorophyll fluorescence observations derived from the Orbiting Carbon Observatory-2 (OCO-2), GOSIF data were obtained after deep learning training to represent the physiologic status of the surface vegetation (Li and Xiao, 2019).

The MODIS NDVI data set (2000−2019) utilized herein was a MOD13A1 product from the NASA data distribution center; this data set has been widely used to study global and regional vegetation changes (Li and Xiao, 2019).

2.6 Data analysis

2.6.1 Inverse distance weighted interpolation analysis

Inverse distance-weighted spatial interpolation is a weighted average interpolation method. This method is based on the principle of similarity outlined in the first law of geography. It is generally considered that the closer the distance between two objects is, the higher their similarity is, and vice versa (Xu et al., 2019). We used the geostatistical analysis tool in ArcGIS 10.4.1 to perform the interpolation calculations (at a spatial resolution of 1 km), cut the study regions after mask processing, and then drew spatial distribution maps of the SOC and SOCD results.

2.6.2 Statistical analysis

The statistical software SPSS 26.0 (SPSS, Chicago, IL, USA) was used to perform the Kolmogorov–Smirnov test, Pearson correlation analysis, one-way ANOVA, and multiple comparisons (Duncan) test to explore the relationships and differences in SOC, SOCD, and environmental factors among test sites. The raw SOCD data in the 0–10 cm and 10–20 cm layers reflected approximately right-skewed distributions.

A redundancy analysis (RDA) (McArdle and Anderson,

2001) was performed with Canoco 5.0 (Biometrics-Plant Research International, Wageningen, The Netherlands) to assess the ability of the environmental variables to explain the SOC contents; the significance of the environmental factors was tested by the Monte Carlo permutation test method. Structural equation modeling (SEM) was used to explore the direct and indirect effects of environmental variables on SOC (Eisenhauer et al., 2015). SEM was conducted with Amos 21.0 (Chicago, Illinois, Illinois Small Water Company, USA). To simplify the model, the soil moisture content (SWC) and pH were selected from the soil chemical factors; the MAP, evapotranspiration (Evap) and elevation (Ele) were selected from the climate factors; and the normalized vegetation index (NDVI), sun-induced chlorophyll fluorescence (SIF) and aboveground biomass (AGB) were selected from the vegetation factors. In Pearson correlation analyses and multimodel reasoning, these factors have been proven to be the main predictors of SOC variance. The criteria for evaluating the SEM fit, such as the P values, χ^2 value, goodness-of-fit index (GFI), and root mean square error of approximation (RMSEA), were adopted in this study by referring to Hooper (Hooper et al., 2008).

3 Results

3.1 Descriptive statistics

Table 1 provides the statistical SOC and SOCD results obtained in the studied desert rangelands. The average SOC and SOCD were 6.81 g·kg^{-1} and 1670.38 g·m^{-2} for the 0–20 cm layer, respectively; the minimum values were 0.05 g·kg^{-1} and 19.23 g·m^{-2}, respectively; the maximum values were 37.13 g·kg^{-1} and 9740.62 g·m^{-2}, respectively; and the CVs were 77.96% and 71.99%, respectively. The average SOC showed a gradual decrease with increasing depth; the contents were 7.62 and 6.13 g·kg^{-1} at depths of 0–10 cm and 10–20 cm, respectively, and the corresponding CVs were 76.50% and 78.87%, respectively. The SOCD also showed a decreasing trend and exhibited large variability between the different soil depths (0–10 cm and 10–20 cm), with averages of 931.57 and 743.49 g·m^{-2}, respectively, and CVs of 72.94% and 74.00%, respectively. Therefore, the SOC and SOCD values of the 0–20 cm layer all showed median variability with CV values between 10% and 100% (Sequeira et al., 2014). The SOC was positively skewed, and the skewness levels of the 0–10 cm and 10–20 cm layers were 1.58 and 1.93, respectively. The SOCD also showed the same trend, with skewness values of 1.91 and 1.86, respectively. As shown in Fig. 2, the 0–10 cm SOC and SOCD were extremely significantly higher than the corresponding values measured at 10–20 cm ($P < 0.01$).

3.2 Comparison of SOC and SOCD values among different desert sites

In the 0–20 cm soil layer (Fig. 3), the highest SOC was measured in the soil desert (8.79 g·kg^{-1}), while the lowest SOC was obtained in the sandy desert (3.20 g·kg^{-1}). The SOC of the soil desert was significantly higher than those of the gravelly desert (1.30 times), gravelly sandy desert (1.38 times), saline desert (1.30 times), and sandy desert (2.75 times). The SOCs of the gravelly desert, gravelly sandy desert, and saline desert were not significantly different ($P > 0.05$) but were all significantly higher than those of the sandy desert. The SOCDs showed the same trends as the SOCs; the largest mean SOCD was obtained in the soil desert (2180.93 g·m^{-2}), while the smallest was obtained in the sandy desert (925.14 g·m^{-2}). The SOCD of the soil desert was significantly higher than those of the gravelly desert (1.39 times), gravelly sandy desert (1.57 times), saline desert (1.42 times), and sandy desert (2.36 times). However, there was no significant difference among the gravelly desert (1569.44 g·m^{-2}), saline desert (1533.54 g·m^{-2}), and gravelly sandy desert (1392.85 g·m^{-2}). The SOC and SOCD differences at depths of 0–10 cm and 10–20 cm among different desert types were similar to those at the 0–20 cm depth.

3.3 Spatial patterns of SOC and SOCD

The spatial patterns of SOC and SOCD were similar in the 0–10 cm, 10–20 cm, and 0–20 cm layers (Fig. 4).

Table 1 Descriptive statistics of the SOC content and density of desert rangelands in northern Xinjiang

Soil layer	Variable	Mean	Med.	SD.	Ske.	Kur.	Min.	Max.	CV/%
0–10 cm	SOC (g·kg^{-1})	7.62	6.18	5.83	1.58	3.57	0.19	37.13	76.50
	SOCD (g·m^{-2})	931.57	774.97	679.49	1.91	6.84	3.23	5749.65	72.94
10–20 cm	SOC (g·kg^{-1})	6.13	4.97	4.83	1.93	6.00	0.05	34.55	78.87
	SOCD (g·m^{-2})	743.49	609.26	550.15	1.86	5.66	3.56	3990.97	74.00
0–20 cm	SOC (g·kg^{-1})	6.81	5.49	5.31	1.74	4.63	0.05	37.13	77.96
	SOCD (g·m^{-2})	1670.38	1390.89	1202.52	1.86	6.20	19.23	9740.62	71.99

Note: Med., SD., Ske., Kur., Min., Max., and CV are abbreviations for the median, standard deviation, skewness, kurtosis, minimum, maximum, and coefficient of variation, respectively.

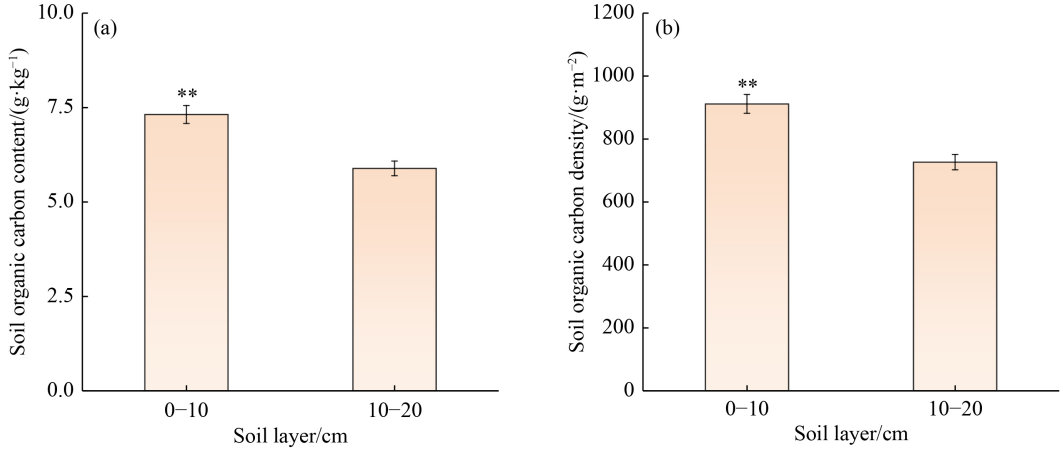

Fig. 2 Comparison of the SOC and SOCD values measured in different soil layers (n = 3162). The ** symbol indicates that the SOC and SOCD values of different soil layers were extremely significant ($P < 0.01$).

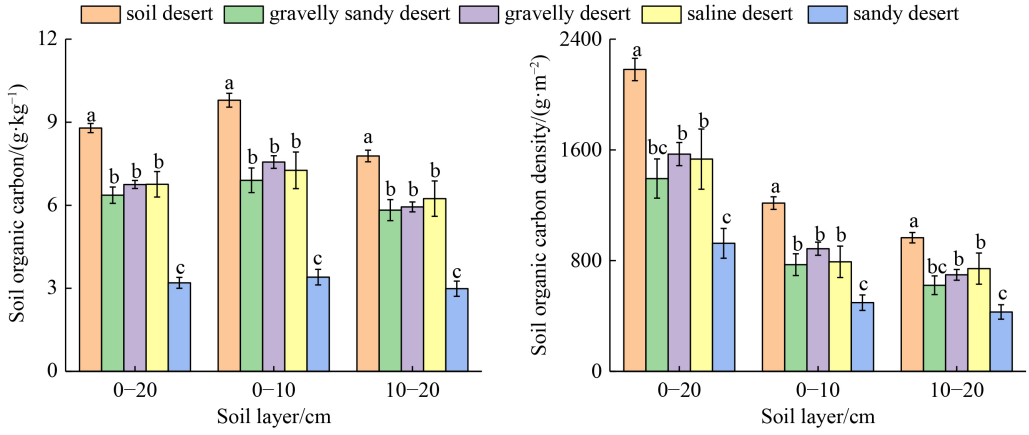

Fig. 3 SOC and SOCD statistics in different deserts (n = 3162). The different lowercase letters indicate significant differences at the 0.05 level.

Overall, both SOC and SOCD at the 0−20 cm layer decreased from south-west to north-east, but clear differences could also be identified. For SOC, high-value areas were distributed in the northern Tacheng region (Emin County), Ili region (Ili valley), western Changji region (Manas County), Urumqi city, and eastern Hami city (Yiwu County); all of these regions belong to the soil desert type. The low-value areas were unevenly distributed and included the sandy desert and gravelly desert sites; these areas were mainly located in the north-western Altay (Habahe County and Jimunai County) and southern Altay (Fuhai County) regions, Karamay city, and Bortala. The SOCD distribution was similar to that of SOC; the high-value areas had relatively abundant precipitation, while low-value areas had sparse precipitation, sparse vegetation, and serious wind erosion. At the same time, the spatial distribution patterns of SOC and SOCD in the 0−10 cm and 10−20 cm soil layers were similar to those in the 0–20 cm soil layer.

Through the accuracy verification of the spatial interpolations, the results showed a significant positive correlation between the measured and predicted values in the 0−20 cm soil layer ($P < 0.01$); the correlation coefficients derived for SOC and SOCD were 0.9302 and 0.9060, respectively (Fig. 5).

3.4 Effects of environmental factors on SOC

To further clarify the effects of climate, soil and vegetation factors on the spatial variations in SOC, a partial redundancy analysis (pRDA) was used to conduct an equation analysis of the SOC variations (Fig. 6). Environmental factors accounted for 37.6% of the variation in SOC in desert rangelands. Vegetation, soil and climate factors accounted for 1.7% ($P < 0.01$), 12.3% ($P < 0.05$), and 15.0% ($P < 0.05$) of the SOC variation, respectively.

The SEM results revealed that soil factors (i.e., SWC and pH) and climatic factors (i.e., MAP, Evap, and Ele) could explain approximately 38% of the total variation in SOC (at 0−20 cm). The model provided good fits (χ^2 = 11.637, df = 7, χ^2/df = 1.662, P = 0.113, GFI = 0.995, RMSEA = 0.035; Fig. 6). The SEM model was fitted successfully when the goodness-of-fit metrics were

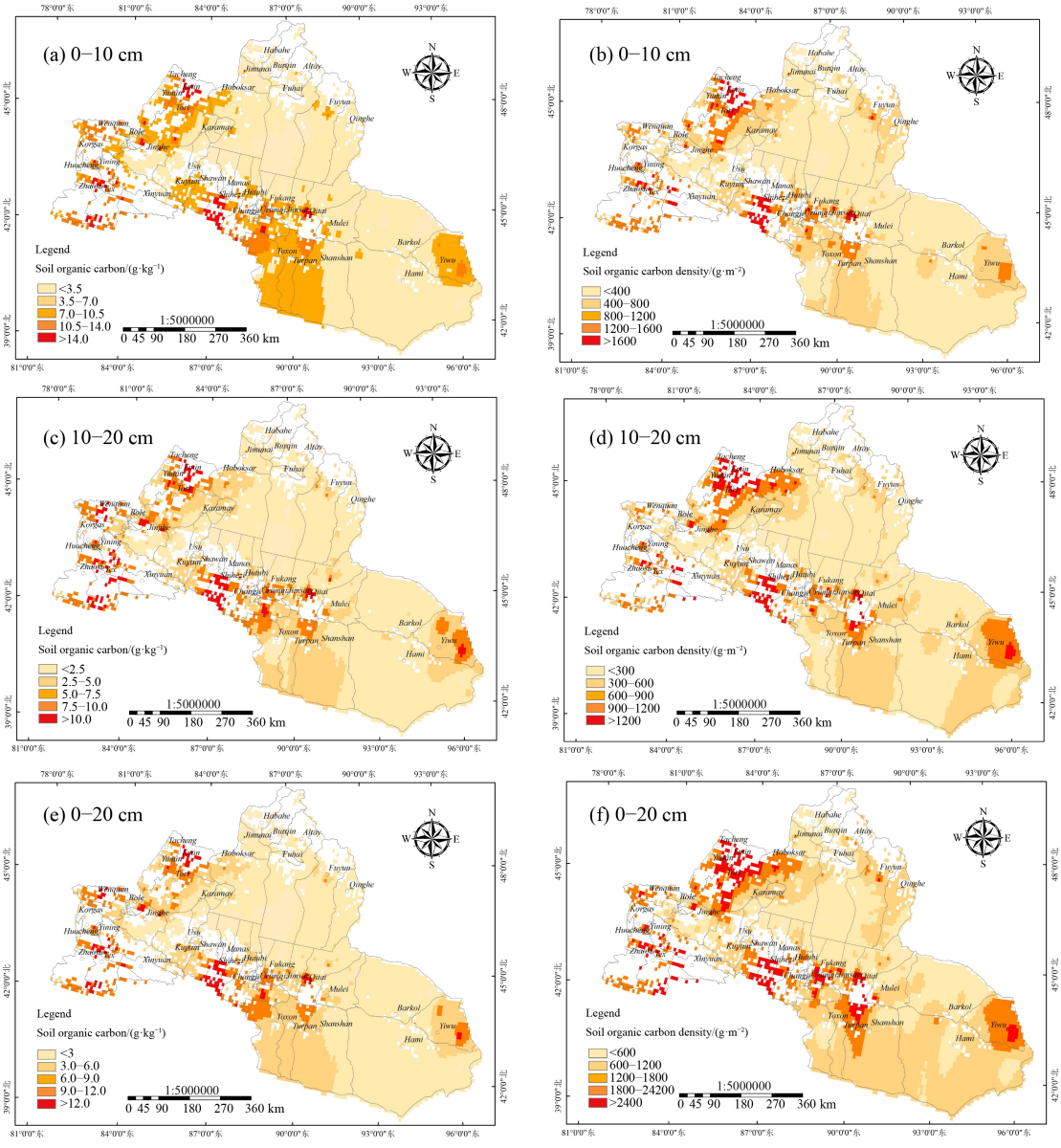

Fig. 4 Spatial patterns of SOC (left) and SOCD (right) in the desert rangelands in northern Xinjiang.

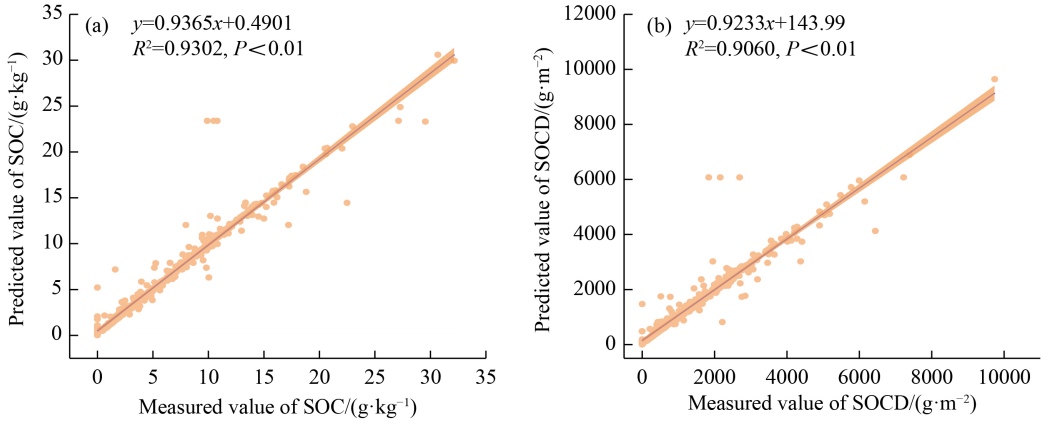

Fig. 5 Linear correlation analysis results between the predicted and measured SOC and SOCD values in surface soils (at a depth of 0–20 cm).

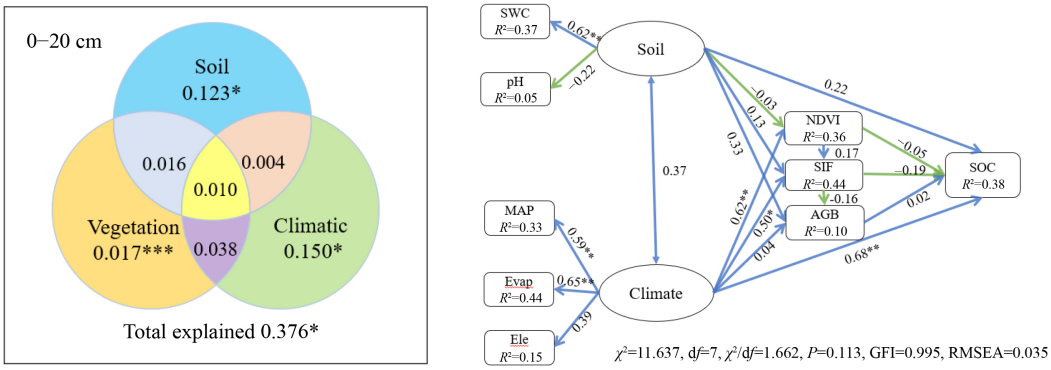

Fig. 6 Driver analysis results of SOC combined with the RDA and SEM results.

satisfied (RMSEA ⩽ 0.085, GFI ⩾ 0.93). The climate factors exerted the strongest direct effect on SOC, with a standardized coefficient of 0.68 at a depth of 0–20 cm ($P < 0.01$). The direct effect coefficient of soil on SOC was 0.22. Regarding the soil properties, the direct influence of the SWC ($r = 0.62$, $P < 0.01$) on SOC was stronger than that of pH ($r = -0.22$, $P > 0.05$). The MAP, Evap, and Ele were all positively correlated with the climate factors, especially MAP ($r = 0.59$, $P < 0.01$) and Evap ($r = 0.65$, $P < 0.01$). Notably, the soil properties were negatively correlated with NDVI ($r = -0.03$) and positively correlated with SIF and AGB, but none of these relations reached a significant level. The effects of climate properties on the SIF ($r = 0.62$, $P < 0.01$) and NDVI ($r = 0.50$, $P < 0.05$) were significant, but the effect of climate properties on AGB was not obvious. None of the vegetation factors (NDVI, SIF, or AGB) had an obvious direct correlation with SOC. None of the vegetation factors (NDVI, SIF, or AGB) had an obvious direct relation with SOC.

In the figure, the single-headed arrows indicate the hypothesized direction of causation. The numbers next to the single-headed arrows show the standardized path coefficients, indicating the effect size of the relationship. The blue arrows represent positive correlations, and the green arrows represent negative correlations; the asterisks indicate statistical significance (**$P < 0.01$; *$P < 0.05$). SWC: soil moisture content; MAP: average annual precipitation; Evap: evapotranspiration; Ele: elevation; NDVI: normalized difference vegetation index; SIF: sun-induced chlorophyll fluorescence; and AGB: aboveground biomass.

4 Discussion

4.1 Spatial distribution characteristics of SOC

The field investigation results showed that the surface SOC of desert rangelands in northern Xinjiang was relatively low; the average SOC content at the 0–20 cm depth was 6.81 g·kg^{-1}. Our results were higher than the SOCs measured in arid regions in Spain (0–30 cm, 2.7 g·kg^{-1}) and during the second soil survey in China (1.78 g·kg^{-1}, $n = 7292$) (Wang and Zhu, 2000; Anta et al., 2020). This may have been because the data of previous studies were obtained from published literature or extrapolated from models, so there was a great deal of uncertainty. However, existing results vary greatly at different regional scales. For example, the SOC in the Taklimakan Desert shelterbelt has been reported to be 1.39 g·kg^{-1} (Ma et al., 2021), and that in a quicksand area was reportedly only 0.60 g·kg^{-1} (Yang et al., 2020); this value was lower than our results. The overall SOC of the Gurbantonggut Desert was found to be 6.00 g·kg^{-1} (Li et al., 2010), which was similar to our results. This phenomenon results mainly from the extremely dry climate conditions in the Taklimakan Desert in southern Xinjiang; in this region, the annual precipitation is only 25.9 mm (Yang et al., 2020) and plant resources are seriously scarce. In comparison, the deserts of northern Xinjiang have more precipitation and richer vegetation types than the Taklimakan Desert. The presence of more precipitation and vegetation lead to increased litter and root exudates, which not only affect the SOC of the soil under the vegetation canopy (Li et al., 2019) but also cause changes in the abiotic environment under the canopy (e.g., in the soil temperature, SWC, and pH) (Yang et al., 2020). Obvious differences were observed among various SOC types in diverse climate regions and even in the same region due to the use of multivariate approaches. Yan et al. (2019) estimated that the SOC values derived by using remote sensing technology were 1.3 times higher than our results (8.70 vs. 6.81 g·kg^{-1}). These differences may have resulted from the different data sources, grassland climate conditions, soil matrices, and litter inputs among different vegetation types affecting the turnover and accumulation of soil carbon (i.e., the presence of different microorganisms (fungi, enzymes, etc.) lead to different decomposition products of fine matter in soils) (Lange et al., 2015; Nicolás et al., 2019).

The topsoil SOCD in the cold desert Ladakh was 2178.25 g·m^{-2}; the surface SOCD of the Nulla Valley

was 2345.00 g·m^{-2}; and that of the Indus Valley was 2011.50 g·m^{-2} (Acharya et al., 2012). In north-west China, the average SOCD was only 723.00 g·m^{-2} (Zhao et al., 2011), and the Loess Plateau surface SOCD was 2640.00 g·m^{-2}. The SOCD measured in our study was 1670.00 g·m^{-2}. The results varied widely by region, and this phenomenon was closely related to the soil matrix and aboveground vegetation types recorded at the sampling sites, thus further indicating the complexity and spatial heterogeneity of desert rangeland environments. As determined from their vertical distributions, SOC and SOCD decreased significantly with increasing depth (Fig. 2). Previous results have shown that the vertical SOC distribution is mainly affected by soil leaching, microbial activities, and mechanical soil disturbances (West et al., 2020). From the perspective of the horizontal distribution, the SOC in Habahe County was the lowest, and this low value was caused by serious wind erosion. The soil matrix in this region mainly consists of sandy soils, and there is no surface runoff. Only a small portion of the precipitation acts to encourage vegetation growth under strong evaporation conditions. The Ili valley had the richest precipitation among the areas considered in this research, with the best vegetation and soil development among the sampled desert types. The areas with the highest SOC and SOCD values were mainly concentrated in the alluvial plains in front of the mountains in the Ili valley (Fig. 4). The increase in local precipitation may be caused by the increase in elevation. Shrubs and herbaceous vegetation can effectively intercept water, promote vegetation growth, and further increase the nutrient inputs from litter and roots (Knapp et al., 2008).

To evaluate the total SOC amount in the soil carbon pool in the desert rangelands of northern Xinjiang, we measured the soil carbon storage in different substrates. The sampled sites could be ordered by their SOCD from high to low as follows: the gravelly desert, saline desert, gravelly sandy desert, and sandy desert. This result was similar to those obtained by other researchers; in past studies, the SOC contents of sandy deserts have been found to be lowest (Li et al., 2010; Ma et al., 2021). This phenomenon is due to the relative scarcity of plant resources in sandy deserts and to the scarce litter, water shortages, and weak microbial activities of these regions making it impossible to replenish the SOC in the soil (Evans et al., 2014). The sampled soil deserts were distributed on the edge of the alluvial fan in front of the Tianshan Mountains; these regions have good soil textures, nutrients, and water contents (Zhao et al., 2011). The soil desert surfaces were densely covered with grasses; the biodiversity was rich in these regions, and the grass root systems were mainly concentrated on the surface, thus affecting the distribution of the bulk density and porosity in the soil profile (Alidoust et al., 2018). The surface soil moisture was largest in the soil desert. Compared with sandy deserts, soil desert vegetation exhibits shallow root systems, small canopies, and high groundwater levels, and surface water resources are abundant in these regions (Chen et al., 2018a), thus resulting in the storage reservoirs having relatively high storage capacities. Soil deserts could be better at providing optimal environmental habitats for microorganisms, enhancing the diversity of microbial communities, and strengthening the stability of the microenvironment, thereby storing SOC (Chen et al., 2018b. This phenomenon was similar to the mechanism by which the dominant species were found to drive the influence of neighboring vegetation (Michalet et al., 2006). The mechanism of this process mainly involved the expansion and creation of realized ecological niches and providing space for more species to accumulate SOC (Crotty and Bertness, 2015). The soil deserts contained more and richer vegetation types than the sandy deserts. Our research results showed that there were significant differences in the SOC changes among different desert subtypes. On the one hand, this phenomenon was related to the microenvironment caused by different rangeland types. Clay occupies a large proportion of soil deserts, and herbaceous plants produce extra organic matter during the soil colonization and development processes, which in turn promote the carbon input to shallow soils (Tong et al., 2018). On the other hand, in arid environments, the carbon input of litter to soils is greater than the carbon output of microbial mineralization, and this imbalance is conducive to SOC accumulation. However, the low SOCs measured in sandy deserts mainly result from litter being easily eroded and blown away by strong winds (Knapp et al., 2010).

4.2 Main factors controlling the SOC distribution

The SOC and SOCD values varied greatly because the surface SOC was easily affected by human activities, vegetation, and soil material changes, especially in terms of the environmental complexity and high spatial heterogeneity (Li and Shao, 2014). This study was based on extensive field sampling of desert rangelands in northern Xinjiang and on a combination of multiple theoretical predictions into a comprehensive model to compare the direct effects (i.e., climatic and soil properties) and indirect effects (i.e., vegetation factors) on SOC in natural ecosystems. The findings of this study suggest two broad generalizations.

First, our results illustrated that the biogeographical patterns of carbon pools in desert rangelands coincide with the MAP and Evap distribution patterns (Fig. 4), thus suggesting that these climate factors play critical roles in shaping the distribution of carbon stocks. As expected, the SEM results supported our hypothesis that precipitation regulates the SOC distribution in desert rangelands (Fig. 6). Furthermore, the results derived

herein implied a soil development relationship that may also relate to climate anomalies. Unlike in other scholars' research, the influence of MAT did not reach a significant level in desert rangelands in this work (Tang et al., 2018). However, the effects of strong evapotranspiration and temperatures were synergistic (i.e., the higher the temperature was, the stronger the effects of soil evaporation and plant transpiration were). The strong positive effect of climate conditions on the desert rangeland SOC storage indicated that precipitation is generally the determinant factor for plant production and microbial respiration in arid areas (Chen et al., 2020). In areas with high precipitation, the stronger the activities of microorganisms and enzymes are, the greater the soil evapotranspiration is. High precipitation values could increase the availability of the respiratory matrix, change the utilization of microbial C, and stimulate microbial growth and activities (Zhao et al., 2016). Moreover, we found that climate conditions, particularly high precipitation, are associated with both higher NDVI and higher SIF values and had consistently positive effects on SOC storage (Chen et al., 2016). However, vegetation (especially shrubs) had a weak impact on SOC. The contribution of vegetation to SOC mainly involved the transport of carbon sources to rhizosphere microorganisms through autotrophic respiration. The sparse vegetation, low community coverage, and few vegetation leaves of new branches on desert rangelands (Su et al., 2015) were also the main reasons for the low correlation found between AGB and SOC in this research. For example, most shrub vegetation (such as *H. ammodendron*) stumps and lignin are difficult for microorganisms to decompose (Artiningsih, 2006), and easily decomposed litter easily moves with the wind, resulting in the poor preservation of SOC.

Second, our results indicated that the direct effects of SOC storage depend on the SWC while excluding the effects of all other factors. This finding suggested that higher SWCs led to better vegetation growth and that the microenvironment also changes accordingly. Then, microbial activity increases to promote the decomposition of litter and carbon inputs (Tunlid et al., 2016), thus improving the SOC storage. An increase in soil moisture also promotes root proliferation. Roots can provide a substrate for microorganisms and stimulate the synthesis of kinase. At the same time, roots provide secretion and oxygen and thus allow enzymes to maintain their normal activities, promote higher turnover, and cope with extreme climatic conditions (Song et al., 2019). In the arid or semiarid western region of Inner Mongolia, the SOC distribution has been found to be mainly limited by the SWC (Song et al., 2019); this was also apparent in our results. The clay, sand, and silt composition ratio in the soil transforms along with a change in soil moisture. Wind erosion destroys the soil aggregate structure, reduces the soil porosity and accelerates the mineralization of SOC to SIC. However, higher AGB levels do not necessarily lead to greater SOC storage in soils (e.g., in sandy desert). For example, the vegetation in the sandy desert rangeland mainly includes *H. ammodendron* and *H. persicum*, and sandy deserts cannot effectively use short-term rainfall to rapidly increase the number of *H. ammodendron* or *H. persicum* individuals to cope with the stress caused by the water and nutrient reductions. Thus, the carbon turnover and release processes are altered (Kušlienė et al., 2014). Therefore, in arid regions, water is the key to providing species diversity and ensuring ecosystem stability.

Based on the SEM results, we considered the MAP, Evap, and SWC to be of equal importance to estimate the direct effects of environmental drivers. However, there was uncertainty due to the complexity of the root biomass and SOC effects in desert rangelands (Tong et al., 2018). The response and feedback relationships between soil properties and rangeland degradation were coupled and indispensable. The response and feedback of soil factors to rangeland degradation coexisted. There were many kinds of soil factors, and their interactions were complex. The causal relationships among these soil factors were not clear in the studied desert rangelands. Thus, when looking for the driving factors of SOC in desert rangelands, more soil factors (such as the soil carbon fraction, soil mechanical composition, soil microorganisms, and soil respiration) should be included from a broader perspective. Quantifying desert SOC and determining its driving factors can provide a scientific basis for sustainability and the "carbon neutrality and carbon peaking" goal. In the future, it is necessary to strengthen the research on technical approaches to earn foreign exchange, optimize ecosystem management measures, and adopt measures to address local conditions.

5 Conclusions

The SOC and SOCD values of desert rangelands in northern Xinjiang were 0.05−37.13 $g \cdot kg^{-1}$ and 19.23−9740.62 $g \cdot m^{-2}$, respectively, with average values of 6.81 $g \cdot kg^{-1}$ and 1670.38 $g \cdot m^{-2}$, respectively. The SOC and SOCD spatial distributions in desert rangelands showed decreasing trends from south-west to north-east. The derived SOC and SOCD data sets both showed moderate spatial variability (71.99%−78.87%). The independent interpretation abilities of climate factors, vegetation factors, and soil factors on the spatial variation in SOC were 15.0%, 1.7%, and 12.3%, respectively. The SEM results showed that vegetation factors have little effect on the spatial distribution of SOC in the desert rangelands. The SOC distribution was controlled not only by climate factors (MAP and Evap) but also potentially by soil factors, especially SWC, in the studied desert rangelands. Overall, the current results enhanced our

understanding of SOC in the arid regions of north-west China and the Central Asia region and provided evidence regarding SOC and climatic-vegetation-soil interactions as well as on the management of desert rangelands as potential sinks in regional or global C budgets.

Acknowledgments This study was funded by the Open Project of Key Laboratory of Xinjiang Uygur Autonomous Region (No. 2022D04003), the National Basic resource survey of China (No. 2017FY100200), the National Natural Science Foundation of China (Grant No. 32060408), and the graduate scientific research and innovation project of Xinjiang Agricultural University (No. XJAUGRI2021003). We wish to acknowledge all participants for their contributions to the field sampling work and laboratory analysis performed in this study. We would also like to thank the editor and the anonymous reviewers for their thoughtful and fruitful feedback on the earlier draft of this manuscript.

Competing interests The authors declare that they have no competing interests.

References

Acharya S, Charan G, Singh N, Srivastava R B (2012). Soil organic carbon sequestration of cold desert Ladakh. Range Manag Agrofor, 33(1): 79–82

Alidoust E, Afyuni M, Hajabbasi M A, Mosaddeghi M R (2018). Soil carbon sequestration potential as affected by soil physical and climatic factors under different land uses in a semiarid region. Catena, 171: 62–71

Artiningsih T (2006). Ligninolytic activity of ganoderma strains on different carbon sources. Biodiversitas (Surak), 7(4): 307–311

Bao S D (2000). Agrochemical Analysis of Soil (3rd Edition). Beijing: China Agricultural Publishing House

Bradford M A, Wieder W R, Bonan G B, Fierer N, Raymond P A, Crowther T W (2016). Managing uncertainty in soil carbon feedbacks to climate change. Nat Clim Chang, 6(8): 751–758

Brecht M, Miralles D G, Lievens H, Van Der Schalie R, De Jeu R A M, Fernández-Prieto D, Beck H E, Dorigo W A, Verhoest N E (2017). GLEAM v3: satellite-based land evaporation and root-zone soil moisture. Geosci Model Dev, 10(5): 1903–1925

Bruun T B, Elberling D E, Neergaard M E, Magid J (2015). Organic carbon dynamics in different soil types after conversion after conversion of forest to agriculture. Land Degrad Dev, 26(3): 272–283

Calvo de Anta R, Luís E, Febrero-Bande M, Galiñanes J, Macías F, Ortíz R, Casás F (2020). Soil organic carbon in peninsular Spain: influence of environmental factors and spatial distribution. Geoderma, 370: 114365

Chen L F, He Z B, Du J, Yang J J, Zhu X (2016). Patterns and environmental controls of soil organic carbon and total nitrogen in alpine ecosystems of northwestern China. Catena, 137: 37–43

Chen S T, Zou J W, Hu Z H, Lu Y Y (2020). Temporal and spatial variations in the mean residence time of soil organic carbon and their relationship with climatic, soil and vegetation drivers. Global Planet Change, 195: 103359

Chen S, Wang W, Xu W, Wang Y, Wan H, Chen D, Tang Z, Tang X, Zhou G, Xie Z, Zhou D, Shangguan Z, Huang J, He J S, Wang Y, Sheng J, Tang L, Li X, Dong M, Wu Y, Wang Q, Wang Z, Wu J, Chapin F S 3rd, Bai Y (2018a). Plant diversity enhances productivity and soil carbon storage. Proc Natl Acad Sci USA, 115(16): 4027–4032

Chen X, Gong L, Li Y M, Zhao J J (2018b). Spatial variation of soil organic carbon and stable isotopes in different soil types of a typical oasis. Environ Sci, 39(10): 4735–4743

Crotty S M, Bertness M D (2015). Positive interactions expand habitat use and the realized niches of sympatric species. Ecology, 96(10): 2575–2582

Delgado-Baquerizo M, Eldridge D J, Maestre F T, Karunaratne S B, Trivedi P, Reich P B, Singh B K (2017). Climate legacies drive global soil carbon stocks in terrestrial ecosystems. Sci Adv, 3(4): e1602008

Eisenhauer N, Bowker M A, Grace J B, Powell J R (2015). From patterns to causal understanding: structural equation modeling (SEM) in soil ecology. Pedobiologia (Jena), 58(2–3): 65–72

Evans R D, Koyama A, Sonderegger D L, Charlet T N, Newingham B A, Fenstermaker L F, Harlow B, Jin V L, Ogle K, Smith S D, Nowak R S (2014). Greater ecosystem carbon in the Mojave Desert after ten years exposure to elevated CO_2. Nat Clim Chang, 4(5): 394–397

Fang J Y, Wang X P, Shen Z H, Tang Z Y, He J S, Yu D, Jiang Y, Wang Z H, Zheng C Y, Zhu J L, Guo Z D (2007). Methods and protocols for plant community inventory. Biodiv Sci, 17(6): 533–548

Germano D J, Rathbun G B, Saslaw L R, Cypher B L, Cypher E A, Vredenburgh L M (2011). The San Joaquin Desert of California: ecologically misunderstood and overlooked. Nat Areas J, 31(2): 138–147

Ghimire R, Bista P, Machado S (2019). Long-term management effects and temperature sensitivity of soil organic carbon in grassland and agricultural soils. Sci Rep, 9(1): 12151

Guan S, An N, Zong N, He Y, Shi P, Zhang J, He N P (2018). Climate warming impacts on soil organic carbon fractions and aggregate stability in a Tibetan alpine meadow. Soil Biol Biochem, 116: 224–236

Hooper D, Coughlan J, Mullen M R (2008). Structural equation modelling: guidelines for determining model fit. Electron J Bus Res Methods, 6(1): 141–146

Hu P L, Liu S J, Ye Y Y, Zhang W, Wang K L, Su Y R (2018). Effects of environmental factors on soil organic carbon under natural or managed vegetation restoration. Land Degrad Dev, 29(3): 387–397

Huang J P, Yu H P, Guan X D, Wang G Y, Guo R X (2015). Accelerated dryland expansion under climate change. Nat Clim Chang, 6(2): 166–171

Huo H, Zhang J, Ma A, Huo J (2018). Progress and prospects of soil carbon cycle in arid desert. J Northwest Forestry U, 33(1): 98–104

Illiger P, Schmidt G, Walde I, Hese S, Kudrjavzev A E, Kurepina N, Mizgirev A, Stephan E, Bondarovich A, Fruehauf M (2019). Estimation of regional soil organic carbon stocks merging classified land-use information with detailed soil data. Sci Total Enviro, 695: 133755

Knapp A K, Briggs J M, Collins S L, Archer S R, Bret-Harte M S,

Ewers B E, Peters D P, Young D R, Shaver G R, Pendall E, Cleary M B (2008). Shrub encroachment in north American rangelands: shifts in growth form dominance rapidly alters control of ecosystem carbon inputs. Glob Change Biol, 14(3): 615–623

Kušlienė G, Rasmussen J, Kuzyakov Y, Eriksen J (2014). Medium-term response of microbial community to rhizodeposits of white clover and ryegrass and tracing of active processes induced by ^{13}C and ^{15}N labelled exudates. Soil Biol Biochem, 76: 22–33

Lal R (2004). Soil carbon sequestration impacts on global climate change and food security. Science, 304(5677): 1623–1627

Lal R (2019). Carbon cycling in global drylands. Curr Clim Change Rep, 5(3): 221–232

Lange M, Eisenhauer N, Sierra C A, Bessler H, Engels C, Griffiths R I, Mellado-Vázquez P G, Malik A A, Roy J, Scheu S, Steinbeiss S, Thomson B C, Trumbore S E, Gleixner G (2015). Plant diversity increases soil microbial activity and soil carbon storage. Nat Commun, 6(1): 6707

Lei T, Feng J, Zheng C, Li S, Wang Y, Wu Z, Lu J, Kan G, Shao C, Jia J, Cheng H (2020). Review of drought impacts on carbon cycling in rangeland ecosystems. Front Earth Sci, 14(2): 462–478

Li C, Li Y, Tang L (2010). Soil organic carbon stock and carbon efflux in deep soils of desert and oasis. Environ Earth Sci, 60(3): 549–557

Li D, Shao M A (2014). Soil organic carbon and influencing factors in different landscapes in an arid region of northwestern China. Catena, 116: 95–104

Li K R, Wang S Q, Cao M K (2003). Vegetation and soil carbon storage in China. Sci China Ser D Earth Sci, 47(1): 49–57

Li X, Xiao J (2019). A Global, 0.05-degree product of solar-induced chlorophyll fluorescence derived from OCO-2, MODIS, and reanalysis data. Remote Sens (Basel), 11(5): 517

Li Y H, Zhao M L, Li F D (2018b). Soil respiration in typical plant communities in the wetland surrounding the high-salinity Ebinur Lake. Front Earth Sci, 12(3): 611–624

Li Y Q, Wang X Y, Niu Y Y, Lian J, Luo Y Q, Chen Y P, Gong X W, Yang H, Yu P D (2018a). Spatial distribution of soil organic carbon in the ecologically fragile Horqin Rangeland of northeastern China. Geoderma, 325: 102–109

Li Y, Wang Y G, Houghton R A, Tang L S (2015). Hidden carbon sink beneath desert. Geophys Res Lett, 42(14): 5880–5887

Liu R T, Zhao H L, Zhao X Y, Zhu F (2013). Effects of cultivation and grazing exclusion on the soil macro-faunal community of semiarid sandy rangelands in northern China. Arid Land Res Manage, 27(4): 377–393

Ma W W, Li G, Wu J H, Xu G R, Wu J Q (2020). Response of soil labile organic carbon fractions and carbon-cycle enzyme activities to vegetation degradation in a wet meadow on the Qinghai–Tibet Plateau. Geoderma, 377: 114565

Ma X, Jin Z Z, Wang Y J, Lei J Q (2021). Effects of shelter forests on soil organic carbon of irrigated soils in the Taklimakan desert. Sustainability (Basel), 13(8): 4535

McArdle B H, Anderson M J (2001). Fitting multivariate models to community data: a comment on distance–based redundancy analysis. Ecology, 82(1): 290–297

Michalet R, Brooker R W, Cavieres L A, Kikvidze Z, Lortie C J, Pugnaire F I, Valiente-Banuet A, Callaway R M (2006). Do biotic interactions shape both sides of the humped-back model of species richness in plant communities? Ecol Lett, 9(7): 767–773

Nicolás C, Martin-Bertelsen T, Floudas D, Bentzer J, Smits M, Johansson T, Troein C, Persson P, Tunlid A (2019). The soil organic matter decomposition mechanisms in ectomycorrhizal fungi are tuned for liberating soil organic nitrogen. ISME J, 13(4): 977–988

Petrie M D, Collins S L, Swann A M, Ford P L, Litvak M E (2015). Grassland to shrubland state transitions enhance carbon sequestration in the northern Chihuahuan Desert. Glob Change Biol, 21(3): 1226–1235

Scharlemann J P, Tanner E V, Hiederer R, Kapos V (2014). Global soil carbon: understanding and managing the largest terrestrial carbon pool. Carbon Manag, 5(1): 81–91

Sequeira C H, Wills S A, Seybold C A, West L T (2014). Predicting soil bulk density for incomplete databases. Geoderma, 213: 64–73

Song Y F, Lu Y J, Guo Z X, Xu X M, Liu T J, Wang J, Wang W J, Hao W G, Wang J (2019). Variations in soil water content and evapotranspiration in relation to precipitation pulses within desert steppe in Inner Mongolia, China. Water, 11(2): 198

Stone R (2008). Have desert researchers discovered a hidden loop in the carbon cycle? Science, 320(5882): 1409–1410

Su Y Z, Wang J Q, Yang R, Yang X, Fan G P (2015). Soil texture controls vegetation biomass and organic carbon storage in arid desert rangeland in the middle of Hexi Corridor region in northwest China. Soil Res, 53(4): 366–376

Tang X, Zhao X, Bai Y, Tang Z, Wang W, Zhao Y, Wan H, Xie Z, Shi X, Wu B, Wang G, Yan J, Ma K, Du S, Li S, Han S, Ma Y, Hu H, He N, Yang Y, Han W, He H, Yu G, Fang J, Zhou G (2018). Carbon pools in China's terrestrial ecosystems: new estimates based on an intensive field survey. Proc Natl Acad Sci USA, 115(16): 4021–4026

Tong L, Zhao B, Wu L M (2018). Effect of grazing on soil organic carbon fractions and soil physical-chemical properties in the desert steppe in Inner Mongolia. Ecolo and Environm Sci, 27(9): 1602–1609

Tunlid A, Floudas D, Koide R, Rineau F (2016). Soil organic matter decomposition mechanisms in ectomycorrhizal fungi. In: Marin F, eds. Molecular Mycorrhizal Symbiosis, 257–275

Wang S Q, Zhu S L (2000). Analysis on spatial distribution characteristics of soil organic carbon reservoir in China. Acta Geogr Sin, 67(5): 533–544

Wang W F, Chen X, Luo G P, Li L H (2014). Modeling the contribution of abiotic exchange to CO_2 flux in alkaline soils of arid areas. J Arid Land, 6(1): 27–36

Wang X Y, Li Y Q, Gong X W, Niu Y Y, Chen Y P, Shi X P, Li W (2019). Storage, pattern and driving factors of soil organic carbon in an ecologically fragile zone of northern China. Geoderma, 343: 155–165

Wang Y H, Liu K X, Wu Z P, Jiao L (2020). Comparison and analysis of three estimation methods for soil carbon sequestration potential in the Ebinur Lake Wetland, China. Front Earth Sci, 14(1): 13–24

Wang Y, Li Y, Ye X, Chu Y, Wang X (2010). Profile storage of organic/inorganic carbon in soil: from forest to desert. Sci Total Environ, 408(8): 1925–1931

West J R, Cates A M, Ruark M, Deiss L, Whitman T, Rui Y (2020). Winter rye does not increase microbial necromass contributions to soil organic carbon in continuous corn silage in North Central US. Soil Biol Biochem, 148: 107899

Xiong L, Liu X, Vinci G, Spaccini R, Drosos M, Li L, Piccolo A, Pan G (2019). Molecular changes of soil organic matter induced by root exudates in a rice paddy under CO_2 enrichment and warming of canopy air. Soil Biol Biochem, 137: 107544

Xu H J, Zhao C Y, Wang X P (2019). Spatiotemporal differentiation of the terrestrial gross primary production response to climate constraints in a dryland mountain ecosystem of northwestern China. Agric For Meteorol, 276-277: 107628

Xu P (1993). Rangeland Resources and Ation in Xinjiang. Urumqi: Xinjiang Science and Technology Health Press (in Chinese)

Yan A, Li B G, Huang F, Zhang W T, Jiang P A, Sheng J D (2019). Distribution and storage of soil organic and inorganic carbon under different ecological zones in Xinjiang, China. Int J Agric Biol Eng, 12(1): 116–125

Yang H T, Wang Z R, Li X J, Gao Y H (2019). Vegetation restoration drives the dynamics and distribution of nitrogen and phosphorous pools in a temperate desert soil-plant system. J Environ Manage, 245: 200–209

Yang Q, Pu H M, Zhao X C, Wang Z W, Chen H, Dong R, Chen Y L, Jin B C (2021). Comparison of field measurement methods for different vegetation coverage of three artificial rangelands. Chin J Appl Environ Biol, 27(1): 220–227

Yang X H, Yang F, Zhou C L, Mamtimin A, Huo W, He Q (2020). Improved parameterization for effect of soil moisture on threshold friction velocity for saltation activity based on observations in the Taklimakan Desert. Geoderma, 369: 114322

Yang Y, Liu B (2019). Effects of planting Caragana shrubs on soil nutrients and stoichiometries in desert steppe of northwest China. Catena, 183: 104213

Zhang X S, Sun S Z, Yong S P, Zhuo Z D, Wang R Q (2007). Vegetation Map of the People's Republic of China (1:1,000,000). Beijing: Geological Publishing House

Zhao B H, Li Z B, Li P, Xu G C, Gao H, Cheng Y T, Chang E H, Yuan S L, Zhang Y, Feng Z H (2017). Spatial distribution of soil organic carbon and its influencing factors under the condition of ecological construction in a hilly-gully watershed of the Loess Plateau, China. Geoderma, 296: 10–17

Zhao C, Miao Y, Yu C, Zhu L, Wang F, Jiang L, Hui D, Wan S (2016). Soil microbial community composition and respiration along an experimental precipitation gradient in a semiarid steppe. Sci Rep, 6(1): 24317

Zhao H L, Zhao X Y, Zhang T H, Zhang X Y, Li Y L, Liu L (2011). Desertification process and its spatial differentation in arid areas of northwest China. J Desert Res, 31(1): 1–8

Zhu H F, Bi R T, Duan Y H, Xu Z J (2017). Scale-location specific relations between soil nutrients and topographic factors in the Fen River Basin, Chinese Loess Plateau. Front Earth Sci, 11(2): 397–406